Otolith shape variation reveals novel stock structure of range-shifting Yellowtail Kingfish (Seriola lalandi lalandi) in Aotearoa New Zealand

Carla Finn[1], Thomas Barnes[2], David Chagne[3], Maren Wellenreuther[3], and Peter Ritchie[1]

[1]Victoria University of Wellington
[2]Earth Sciences New Zealand
[3]The New Zealand Institute for Bioeconomy Science Limited (Bioeconomy Science Institute – formerly Plant & Food Research)

January 06, 2026

Abstract

Climate-driven range expansion is reshaping species distributions worldwide, altering population connectivity and complicating stock assessment in many marine taxa. In Aotearoa New Zealand, Yellowtail Kingfish (Seriola lalandi lalandi) have extended southward from their historically northern distribution, prompting renewed questions about stock boundaries and connectivity across the range. Here, we present the first comprehensive evaluation of sagittal otolith shape variation in this species and assess whether otolith morphology can serve as an indicator of ongoing range-expansion dynamics. We analysed otoliths from 112 individuals collected across five regions using wavelet-based contour descriptors and traditional shape indices to test for spatial structure and signatures of expansion. Wavelet-based contour descriptors differed significantly between Auckland West—the traditional home range of Yellowtail Kingfish— and all other sampled regions, which represent the species' ongoing range expansion. Classification analyses further achieved the highest assignment success for Auckland West fish, underscoring the utility of otolith shape for identifying individuals from this historic northern range. Together, these findings demonstrate the value of otolith morphology as a tool for delineating stock structure and supporting adaptive fisheries management under accelerating climate-driven distributional shifts.

Otolith shape variation reveals novel stock structure of range-shifting Yellowtail Kingfish (*Seriola lalandi lalandi*) in Aotearoa New Zealand

Carla H. Finn*[1], Thomas C. Barnes[2, 5], David Chagné[3], Maren Wellenreuther[3,4], and Peter Ritchie[1]

[1]Te Herenga Waka – Victoria University of Wellington, Aotearoa New Zealand
[2]Earth Sciences New Zealand, Aotearoa New Zealand
[3]Bioeconomy Science Institute, Nelson, Aotearoa New Zealand
[4]University of Auckland, Aotearoa New Zealand
[5] Institute of Marine and Antarctic Studies, University of Tasmania, Hobart, Tasmania, Australia

Abstract

Climate-driven range expansion is reshaping species distributions worldwide, altering population connectivity and complicating stock assessment in many marine taxa. In Aotearoa New Zealand, Yellowtail Kingfish (*Seriola lalandi lalandi*) have extended southward from their historically northern distribution, prompting renewed questions about stock boundaries and connectivity across the range. Here, we present the first comprehensive evaluation of sagittal otolith shape variation in this species and assess whether otolith morphology can serve as an indicator of ongoing range-expansion dynamics. We analysed otoliths from 112 individuals collected across five regions using wavelet-based contour descriptors and traditional shape indices to test for spatial structure and signatures of expansion.

Wavelet-based contour descriptors differed significantly between Auckland West— the traditional home range of Yellowtail Kingfish— and all other sampled regions, which represent the species' ongoing range expansion. Classification analyses further achieved the highest assignment success for Auckland West fish, underscoring the utility of otolith shape for identifying individuals from this historic northern range. Together, these findings demonstrate the value of otolith morphology as a tool for delineating stock structure and supporting adaptive fisheries management under accelerating climate-driven distributional shifts.

Keywords: Range expansion, climate change, population structure, Seriola, fisheries.

1 Introduction

Ongoing ocean warming is facilitating the poleward redistribution of marine species, with numerous taxa shifting their ranges polewards in response to shifting thermal habitats (Poloczanska et al., 2013). In Aotearoa New Zealand, rising sea surface temperatures have coincided with a Southward Range Expansion (SRE) of Yellowtail Kingfish (*Seriola lalandi lalandi*) over the past decade. Once largely restricted to the Northern half of the North Island - its Northerly Historic Range (NHR)—this warm-temperate species is now increasingly reported further south, prompting debate about whether current management boundaries are still fit for purpose (Fisheries New Zealand, 2020).

Understanding the dynamics of this expansion requires consideration of the stock concept, which is fundamental to modern fisheries management, including in Aotearoa New Zealand, where the quota management system the QMS has been deployed since 1986 (Cryer et al., 2016). This provides a useful lens through

*Corresponding author: carla.finn@vuw.ac.nz, Victoria University of Wellington Level 2, Te Toki a Rata Building, Gate 7, Kelburn Parade, Wellington, NZ 6012

which to evaluate the implications of this SRE. A stock is defined as a reproductively or demographically distinct unit of fish, defined based on genetic, phenotypic, environmental, and/or harvest-related characteristics (Ihssen et al., 1981; Carvalho & Hauser, 1994) - also, see Waples & Gaggiotti (2006). Stocks are typically characterised by limited gene flow, distinct growth and recruitment dynamics, and thus may respond independently to exploitation (Cadrin et al., 2013). Correctly identifying the boundaries and connectivity of stocks is critical because misalignment can lead to management strategies that can be problematic for the design of effective, spatially relevant management strategies.

For Yellowtail Kingfish, a key uncertainty is whether southern occurrences represent the permanent establishment of new, demographically independent stocks (i.e. new stock components), or whether they are temporary excursions by individuals that ultimately return to the NHR. This distinction has important implication for connectivity, local exploitation risks and the potential for adaptive change. Distinguishing "expander" individuals from NHR residents would provide a powerful way to track the frequency, direction, and persistence of range expansion events.

Otoliths provide a useful intrinsic marker for addressing this gap. In teleost fishes, three pairs of otoliths—sagitta, asteriscus, and lapillus- reside in the inner ear and play critical roles in balance and hearing (Das, 1994). The sagittal otolith, the largest of the three, is commonly used in ecological and stock structure studies. Otolith shape is determined by both genetic (Berg et al., 2018; Vignon & Morat, 2010) and environmental influences, including temperature (Mahé et al., 2019; Geladakis et al., 2022), salinity (Clark et al., 2021), diet (Mille et al., 2016; Park et al., 2023), and water depth (Gauldie & Crampton, 2002). Shape divergence among fish stocks can increase with geographic distance and genetic differentiation (Vignon & Morat, 2010), making otolith morphology a useful marker for identifying partially isolated stocks subjected to distinct environmental conditions (Park et al., 2023; Libungan et al., 2015), reviewed in Nazir & Khan (2021).

The development of digital imaging technologies and mathematical descriptors, such as fourier and wavelet, has significantly enhanced the ability to quantify and compare otolith shape (Libungan & Pálsson, 2015; Park et al., 2023). These methods allow for high-resolution characterization of otolith contours, facilitating the detection of subtle phenotypic divergence among stocks.

Here, we present the first evaluation of otolith shape for Yellowtail Kingfish in Aotearoa New Zealand. Using wavelet descriptors, in addition to with shape and size indices, to test whether otolith morphology can distinguish between Yellowtail Kingfish from both the NHR and areas within the SRE across five sampling regions of Aotearoa New Zealand. Specifically, our objectives were to: i) assess whether otolith shape varies among Yellowtail Kingfish stocks across five regions, and ii) evaluate whether these differences correspond to, and also enable accurate discrimination between, the NHR and the areas associated with the SRE.

Box 1.1: Abbreviations used in this study

General Abbreviations

NHR – *Northern Historic Range.* The traditional range observed for Yellowtail Kingfish, i.e., the northern half of the North Island in Aotearoa New Zealand.

SRE – *Southward Range Expansion.* The non-traditional poleward shift observed for Yellowtail Kingfish; consists of 'expansion/expander'-associated individuals.

Sampling Area Abbreviations

AKW – *Auckland West.*
CEW – *Central West.*
CHA – *Challenger Plateau.*
SOU – *Southland.*
BPLE – *Bay of Plenty.*

2 Methods

A total of 112 Yellowtail Kingfish individuals were collected from five sampling areas across Aotearoa New Zealand. The sampling locations are provided in Figure 1. Abbreviations for the sampling areas are provided in Box 1.1.

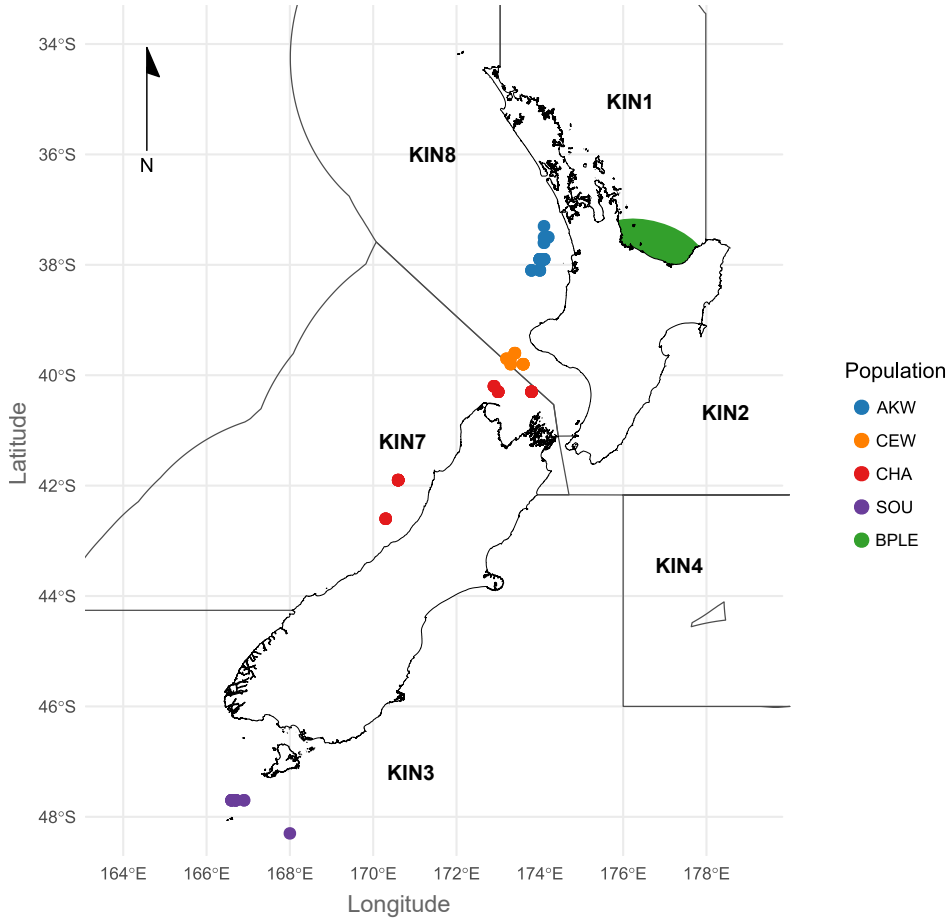

Figure 1: Map showing the locations of the individual Kingfish per sampling area. Note that the precise location of BPLE cannot be released due to confidentiality reasons; therefore, the general sampling area has been provided. The map has been superimposed onto the Yellowtail Kingfish Fishery Management areas for NZ, as provided by the Ministry of Primary Industries (MPI, 2002). Abbreviations for the sampling areas are provided in Box 1.1. Sampling area counts are provided in Table 1.

Individuals were caught using commercial trawl targeting jack mackerel (sampling areas CHA, AKW, CEW and SOU), and angling (sampling area BPLE). Sagittal otoliths were extracted from each individual by onboard scientific observers. Due to the brittle nature of otoliths, either the left or right otolith was occasionally damaged during extraction. Paired left or right otoliths were successfully obtained from 29 individuals and were used for bilateral asymmetry analysis. Based on the results from this analysis, where a right otolith was unavailable, a mirror-reflected image of the left otolith was substituted for analyses; this method is also demonstrated throughout the literature i.e., (Aneesh Kumar et al., 2017; Ndjamba et al., 2022), and is similarly demonstrated with likewise results for the genus *Seriola* in Crandall et al. (2013).

2.1 Otolith imaging

High-resolution images of the otoliths were obtained using a Nikon Instruments Inc., Tokyo, Japan) coupled with NIS-Elements software, version 5.3 (Nikon Instruments Inc., Tokyo, Japan). Otoliths were positioned on

Table 1: Numbers of individuals used in this study, by year and sampling area. Abbreviations for the sampling areas are provided in Box 1.1.

Year	CHA	AKW	BPLE	CEW	SOU	Total
2014		13	24			37
2019	20	13		6	1	40
2021		1		9		10
2023	13					13
2024					12	12
Total	33	27	24	15	13	112

a dark microscope plate with the distal face oriented upward. All images were taken at a fixed magnification of 10x and saved in JPEG format. Before outline extraction, all images were processed in ImageJ version 1.54g (Schneider et al., 2012). This involved manually removing debris to avoid distortion of the otolith outline, enhancing contrast to achieve white otoliths against a black background, and centering the otolith within the frame (as demonstrated in Figure 2). These steps were necessary to optimize outline detection by the ShapeR package.

Figure 2: **Demonstrating the otolith imaging process.** A) represents the raw otolith image, B) represents the edited and centered otolith image, as edited using ImageJ (high-contrast white denoting the otolith area), and C) represents the outline function of the `shapeR` package (the red line denotes the perimeter). The scale bar in each image is 1mm.

2.2 Otolith shape outline detection and reconstruction

Outlines of otoliths were extracted using the `detect.outline()` function in the `ShapeR` package (version 1.0.1) (Libungan & Pálsson, 2015) in `RStudio` (R version 4.4.1) (R Core Team, 2019). A threshold value of 0.3 was applied to distinguish the otolith boundary. Each detected outline was saved as a PNG image and manually inspected to check that the detected outline followed the contour of the otolith edge, as expected (for example, see Figure 1). Following smoothing (100 iterations), shape descriptors were computed using both Wavelet and Elliptic Fourier (EF) transformations. All shape descriptors were standardized to fish total length (cm) using the `stCoefs()` function with Bonferroni adjustment enabled. No coefficients were excluded after standardisation for any analysis.

Reconstruction accuracy was assessed using the `estimate.outline.reconstruction()` function. Wavelet coefficients at level 9 reconstructed outlines with 100% accuracy (0% deviation), whereas EF harmonics achieved 98.8% at level 15 (Appendix Figure S2). As a result, all Wavelet coefficients were retained for subsequent shape analyses.

2.3 Otolith contour analyses

Wavelet coefficients were used to visualize otolith shape differences among sampling areas via Canonical Analysis of Principal Coordinates (CAP) (Anderson & Willis, 2003). Ordination was performed using the `capscale()` function in the `vegan` package with sampling area as the constraining variable and Euclidean

distances among standardized Wavelet coefficients as the response. The CAP model generates constrained axes, representing the portion of multivariate shape variation explained by sampling area. Significance of the constrained axes was evaluated using a permutation-based ANOVA. Pairwise comparisons between sampling areas were tested using the `PairwiseAdonis` R package (version 0.4.1) (Arbizu, 2020) with 999 permutations and Holm correction. To verify the assumption of homogeneity of multivariate dispersions, `betadisper()` and `permutest()` were applied from the `vegan` R package (version 2.6-6.1) (Oksanen et al., 2016), followed by Tukey's HSD post-hoc testing when applicable.

2.4 Otolith indices

Otolith size indices - length (OL, mm), height (OH, mm), perimeter (OP, mm), and area (OA, mm^2) -were computed using `ShapeR`. Shape-related indices were derived from these dimensions using formulas adapted from (Park et al., 2023), and included: form factor (FF), aspect ratio (AR), ellipticity (E), circularity (C), roundness (RO) and rectangularity (RE) (Table 2).

Table 2: Analytical expressions used to calculate otolith shape indices.

Index (Abbreviation)	**Equation**
Circularity (C)	$\text{Perimeter}^2/\text{Area}$
Rectangularity (RE)	$\text{Area}/(\text{Length} \times \text{Width})$
Roundness (RO)	$4 \times \text{Area}/(\pi \times \text{Length}^2)$
Aspect Ratio (AR)	Length/Width
Form Factor (FF)	$4\pi \times \text{Area}/\text{Perimeter}^2$
Ellipticity (E)	$(\text{Length} - \text{Width})/(\text{Length} + \text{Width})$

To account for allometric scaling with fish sizes (see Results), all indices were standardized using log-log regression against total fish length (Lleonart et al., 2000) with the equation:

$$M_s = \exp\left(\log(M) + b\left[\log(\bar{L}) - \log(L)\right]\right) \tag{1}$$

Where:

- M is the raw measurement (e.g., otolith area, shape index),
- M_s is the standardized measurement,
- L is the total length of the individual fish,
- $\bar{L}$ is the mean total length across all individuals,
- b is the allometric scaling coefficient, estimated as the slope from the regression of $\log(M) \sim \log(L)$.

2.5 Preliminary tests used in this study

Preliminary tests were conducted to assess the suitability of data before the sampling area differentiation testing.

2.5.1 Prior test 1: left-right otolith asymmetry

To assess bilateral asymmetry, standardized shape indices were compared between left and right otoliths for 29 individuals (58 otoliths total). Normality of paired differences was tested using the Shapiro–Wilk test. If normality was satisfied, a paired t-test was conducted; otherwise, the Wilcoxon signed-rank test was applied. Holm-adjusted p-values were calculated to account for multiple testing. There were no significant results between left and right otoliths (see Appendix Table S1).

To evaluate whether shape–length relationships differed by side, ANCOVA models were constructed for each shape index. A full model including an interaction term (side $\times$ *length_cm*) was compared against a reduced model using a likelihood ratio test. No interaction terms were statistically significant after correction (see Appendix Table S2).

Based on these tests, where the right otolith was not available for a given individual, a mirror-imaged left otolith was used.

2.5.2 Prior test 2: temporal comparison of 2014 vs 2019 AKW samples

To assess potential temporal variation in otolith morphology within the AKW sampling region, standardized Wavelet coefficients were evaluated by comparing specimens collected in 2014 (n = 13) with those obtained in 2019 (n = 13), reflecting the five-year interval between available AKW samples. Otolith Shape ordination was performed as already described in 2.3 Otolith contour analyses. No significant differences in shape profiles were detected between years (PERMANOVA: F = 0.627, R^2 = 0.026, p = 0.781), and group dispersions were homogenous (PERMDISP: F = 0.007, p = 0.943). Consequently, AKW samples from both years were pooled in further analyses (also see Appendix Figure S1).

2.6 Stock-level differences

2.6.1 Otolith contour analysis

To assess spatial variation in otolith shape among sampling regions, we applied the same wavelet descriptor procedure described in 2.3 Otolith contour analyses. Due to a significant violation of dispersion homogeneity in the BPLE sampling area, BPLE was excluded from PERMANOVA testing (see results 3.2.1 Shape contour analysis).

To evaluate the discriminatory power of otolith shape for assigning individuals to sampling area of origin, we performed a Linear Discriminant Analysis (LDA) using standardized Wavelet coefficients as predictors. The LDA was implemented using the `MASS` package (version 7.3-60) (Kemp, 2003) with leave-one-out cross-validation (LOOCV).

2.6.2 Otolith shape indices analysis

To assess shape and size indices differences, we applied the same shape indices procedure described in 2.4 Otolith indices. Each otolith size and shape index were assessed for normality using the Shapiro–Wilk test. Variables that violated the assumption of normality ($p < 0.05$) were subsequently categorized for non-parametric testing. Homogeneity of variance across sampling areas was assessed for each index using Levene's test (as implemented in the `rstatix` R package, (version 0.7.2) (Kassambara, 2021)

Based on these assumptions, the following analytical approach was used:

- For indices that met both normality and homogeneity assumptions, a one-way ANOVA was conducted, followed by Tukey's Honest Significant Difference (HSD) test for post-hoc pairwise comparisons.
- For indices that were normally distributed but violated the homogeneity of variance assumption, Welch's ANOVA was used, followed by Games–Howell post-hoc tests.
- For indices that failed normality, a Kruskal–Wallis test was performed, followed by Dunn's test for post-hoc pairwise comparisons with Holm-adjusted p-values (as implemented in the `rstatix` R package).

2.7 Data availability

All data for repeating this analysis, including the code used, can be found at: `https://doi.org/10.5061/dryad.gmsbcc335`

For reviewers, the following link should be used: `http://datadryad.org/share/LINK_NOT_FOR_PUBLICATION/SJlLJ5yrKIA4WzoD3PSKbKz2yhLHGZupBhb_tGaDiro`

2.7.1 Packages and scripts in this study

All statistical tests were as implemented either in base packages belonging to `R` version 4.4.1 (base R) (R Core Team, 2019), or otherwise in packages specified in-text. Other packages used for purpose of data wrangling are: `dplyr` (version 1.1.4) (Hadley Wickham et al., 2020) `tidyr` (version 1.3.1) (Wickham et al., 2024) `ggplot2` (version 3.5.2) (Wickham, 2011).

3 Results

A total of 112 Yellowtail Kingfish individuals, sampled across five sampling areas, were included in the otolith analysis. These sampling sites span a longitudinal gradient across Aotearoa New Zealand (Figure 1; abbreviations for the sampling areas provided in Box 1.1.). Sample composition was as follows: 27 BPLE individuals (75–123.5 cm), 15 CEW individuals (71–90 cm), 33 CHA individuals (67–112 cm), 13 SOU individuals (90-109 cm), and 27 AKW individuals (67–87 cm).

3.1 Otolith indices

Descriptive statistics for otolith size and shape indices across the five sampling locations are presented in Table 3. Neither parametric nor non-parametric tests revealed significant differences in any single size or shape index across sampling areas, suggesting that no individual metric independently explains the observed divergence.

3.2 Average shape contours

Average otolith outlines based on wavelet coefficients (0°–360°) showed subtle differences in mean shape among sampling areas, particularly near 90° and 180°, corresponding to the antirostrum. CEW individuals exhibited a more rounded and elevated antirostrum, whereas BPLE displayed a flatter, less inflected contour. In contrast, AKW individuals had a sharply inflected and dorsally depressed antirostrum, positioned lower than other groups (Figure 3).

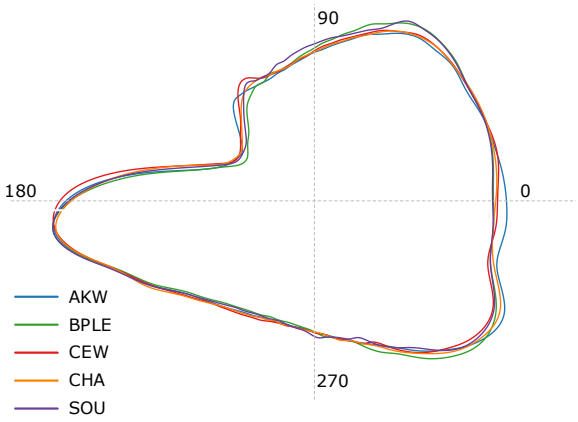

(a) Average otolith contour, with angles given in degrees. Contours are overlaid for comparison.

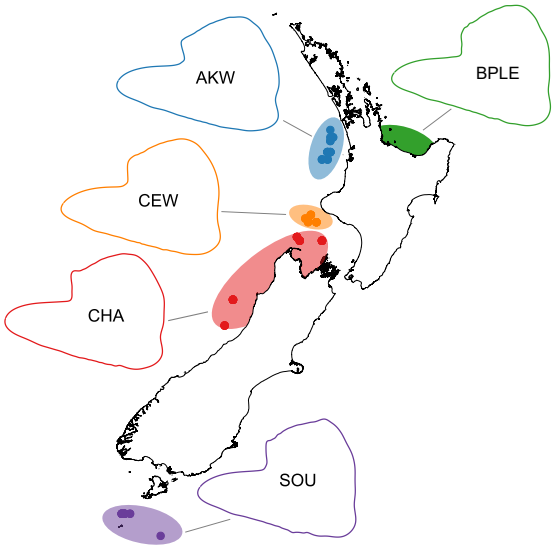

(b) Average otolith contour for each sampling area. Points represent individuals. Note that the precise location of BPLE can not be released due to confidentiality reasons; therefore, the general sampling area has been provided.

Figure 3: Average otolith contours, as generated using the `shapeR` package, which utilises wavelet coefficients. Coloured by sampling area. Abbreviations for the sampling areas are provided in Box 1.1.

3.2.1 Shape contour analysis

Wavelet coefficients were analysed using canonical analysis of principal coordinates (CAP). Prior to permutation tests, we assessed the homogeneity of multivariate dispersions using `betadisper()` followed by `permutest()`, which indicated significant differences among groups ($p = 0.002$). Post-hoc Tukey's HSD tests revealed that the BPLE sampling area exhibited significantly greater dispersion than both AKW ($p = 0.001$)

Table 3: Summary of otolith size and shape indices across sampling locations. Abbreviations for the sampling areas are provided in Box 1.1. Values are reported as Min–Max (Mean ± SD).

	Min–Max (Mean ± SD)				
Standardised Variables	AKW	BPLE	CEW	CHA	SOU
Aspect Ratio	2.40–3.27 (2.76 ± 0.22)	2.19–3.27 (2.70 ± 0.36)	2.37–3.23 (2.76 ± 0.26)	2.22–3.21 (2.72 ± 0.23)	2.18–3.33 (2.73 ± 0.36)
Circularity	27.34–38.19 (33.52 ± 2.78)	29.55–44.53 (35.46 ± 3.43)	28.20–40.02 (31.73 ± 3.11)	25.44–39.86 (33.56 ± 3.15)	26.91–40.95 (32.92 ± 3.54)
Ellipticity	0.41–0.53 (0.45 ± 0.03)	0.37–0.46 (0.41 ± 0.03)	0.41–0.52 (0.45 ± 0.03)	0.38–0.52 (0.45 ± 0.04)	0.35–0.53 (0.41 ± 0.05)
Form Factor	0.33–0.46 (0.39 ± 0.03)	0.28–0.57 (0.42 ± 0.26)	0.31–0.44 (0.38 ± 0.03)	0.32–0.49 (0.41 ± 0.03)	0.31–0.43 (0.38 ± 0.03)
Rectangularity	0.45–0.53 (0.48 ± 0.02)	0.51–0.69 (0.60 ± 0.04)	0.45–0.58 (0.52 ± 0.03)	0.36–0.63 (0.52 ± 0.06)	0.52–0.63 (0.56 ± 0.04)
Roundness	0.21–0.31 (0.27 ± 0.04)	0.22–0.37 (0.29 ± 0.04)	0.23–0.30 (0.27 ± 0.02)	0.23–0.38 (0.28 ± 0.03)	0.22–0.34 (0.26 ± 0.03)
Otolith Area	11.51–21.63 (13.97 ± 2.21)	11.40–17.57 (14.55 ± 1.80)	11.46–15.19 (13.19 ± 0.99)	10.66–17.46 (12.47 ± 1.89)	10.68–15.79 (13.66 ± 1.41)
Otolith Length	7.14–8.81 (8.69 ± 0.50)	6.48–10.01 (8.20 ± 0.86)	7.43–8.88 (7.93 ± 0.41)	6.91–9.26 (8.15 ± 0.57)	6.48–9.10 (8.07 ± 0.57)

and CEW ($p = 0.038$) (see Appendix Table S3), thereby violating the assumption of dispersion homogeneity required for valid ANOVA. Consequently, BPLE was excluded from subsequent analyses.

After excluding BPLE, homogeneity of dispersion among remaining groups was no longer significant ($p = 0.075$).

The CAP model showed a statistically significant effect of sampling area on otolith shape (Permutation test: $F = 2.13$, $p = 0.001$), explaining 7.1% of the total variation in shape space. Sequential term testing confirmed sampling area as a significant explanatory variable ($p = 0.002$). Axis-wise testing revealed that only the first canonical axis (CAP1) contributed significantly to group separation ($p = 0.001$), while CAP2 and CAP3 were non-significant. Thus, shape variation among locations was primarily captured along CAP1 (Figure 4).

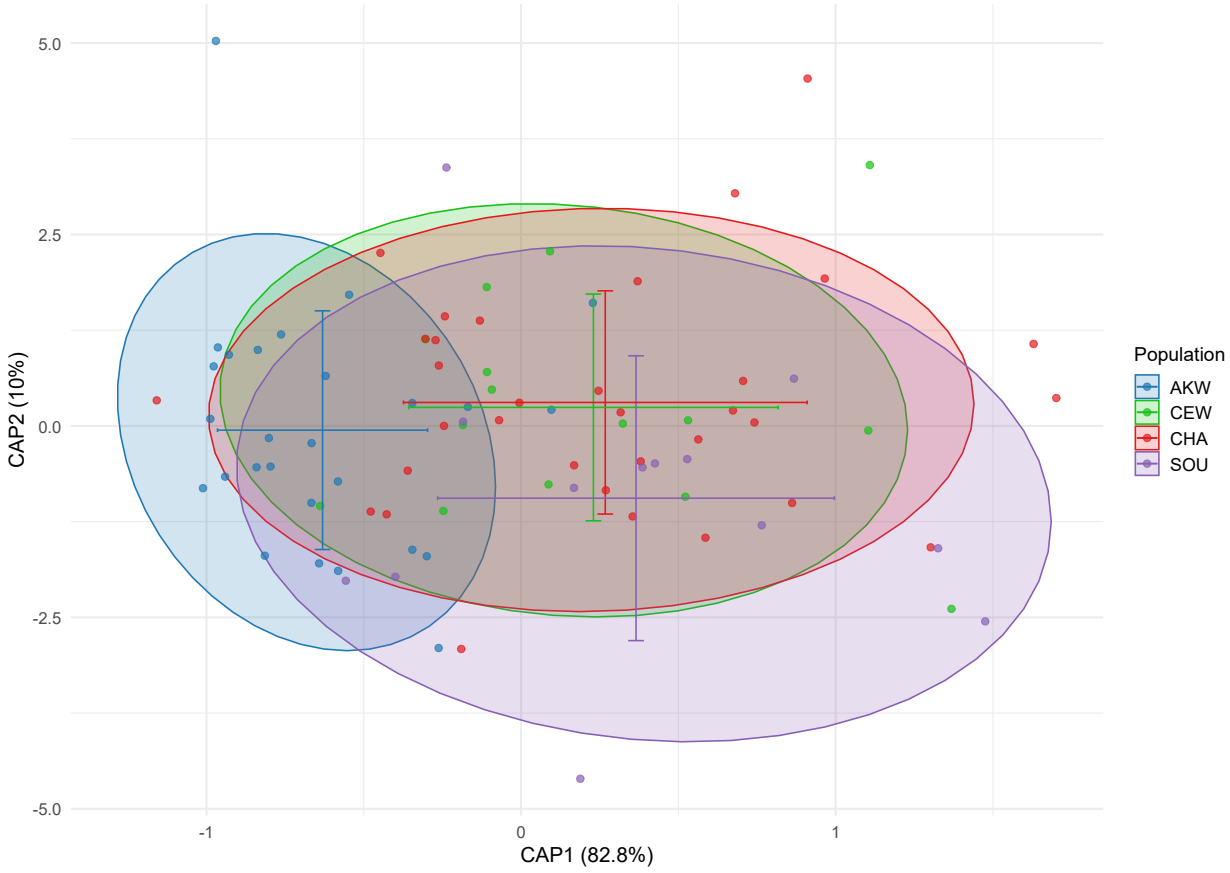

Figure 4: Canonical analysis of principal coordinates (CAP) using Euclidean distances of standardized wavelet coefficients, shown for four Yellowtail Kingfish *S. lalandi lalandi* sampling areas in Aotearoa New Zealand. BPLE was excluded due to high within-group dispersion. Points represent individuals; crosses indicate group centroids with bars showing ±1 SD. Ellipses denote 95% confidence intervals under multivariate normality.

Pairwise PERMANOVA comparisons (Table 4) revealed significant shape differences between AKW and each of CEW, CHA, and SOU (adjusted $p = 0.006$). No significant differences were observed among CEW, CHA, or SOU (adjusted $p = 1.000$), indicating that AKW is the primary driver of inter-sampling area shape divergence.

Table 4: Pairwise PERMANOVA comparisons of wavelet-based otolith shape among sampling areas, showing F-statistics, R^2, and raw and Holm-adjusted p-values. Asterisks indicate statistically significant differences ($p < 0.05$). Abbreviations for the sampling areas are provided in Box 1.1.

Comparison	F-value	R^2	Raw p-value	Holm-adjusted p	Significant
AKW vs CEW	3.15	0.073	0.001	0.006	*
AKW vs CHA	4.50	0.072	0.001	0.006	*
AKW vs SOU	3.30	0.080	0.001	0.006	*
CEW vs CHA	0.46	0.010	0.941	1.000	
CEW vs SOU	0.53	0.020	0.871	1.000	
CHA vs SOU	0.58	0.013	0.824	1.000	

Classification using leave-one-out cross-validation (LOOCV) (Figure 5) resulted in an overall correct assignment rate of 45.5%. The highest classification success was observed for AKW individuals (63%), consistent with the distinct separation of this group observed in the CAP ordination analysis. In contrast, classification performance was lowest for CEW and SOU, with only 20% and 7.7% of individuals correctly assigned, respectively.

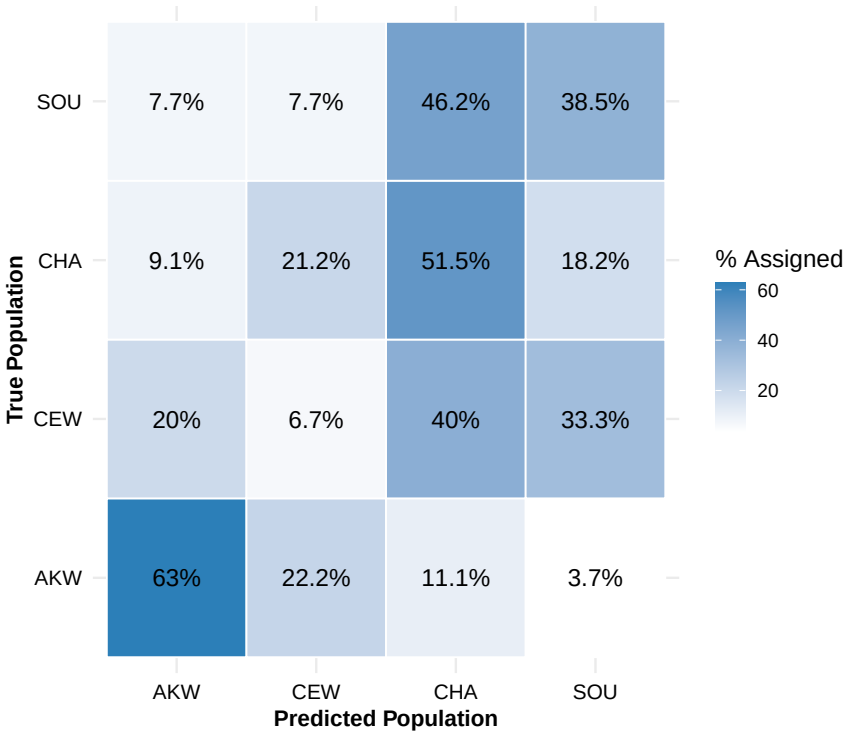

Figure 5: LOOCV Confusion Matrix – Otolith Shape Classification based on standardized wavelet coefficients (LDA model). Overall correct assignment rate of 45.5%. Abbreviations for the sampling areas are provided in Box 1.1.

4 Discussion

This otolith shape study provides evidence of stock-level structure in Yellowtail Kingfish *(Seriola lalandi lalandi)*. The distinctiveness of Auckland West (AKW) otolith contours, together with the 63% correct classification rate for AKW individuals, suggests partial demographic separation within the NHR. By contrast, the relative homogeneity among Central West (CEW), Challenger (CHA), and Southland (SOU) supports the interpretation that southern fish represent recent or ongoing expansion poleward, rather than established, independent stocks. These patterns are consistent with observations of Yellowtail Kingfish catches now extending further south than historically reported in Aotearoa New Zealand (Ministry for Primary Industries, 2019).

Based on this information, we predict an increasing persistence in the SRE regions (i.e., poleward shift) in Aotearoa New Zealand, a pattern that has likewise been predicted via modelling for Yellowtail Kingfish in Southeastern Australia (Champion et al., 2018).

4.1 Classifying range expansions in Yellowtail Kingfish

The Auckland West (AKW) sampling area exhibited a uniquely distinct otolith contour relative to all other regions. This is notable given that stock differentiation in this region, for this species, has not previously been reported. The observed divergence at AKW may indicate ecological and demographic separation, but further confirmation will require supporting ecological or genomic evidence. Such divergence is unexpected in pelagic species like Yellowtail Kingfish, which typically exhibit weak spatial structuring due to high dispersal potential, large effective population sizes, and low site fidelity. However, it has been demonstrated that under climate-change scenarios, climate-driven range shifts are rapid in coastal-pelagic fishes, such as Yellowtail Kingfish (Champion et al., 2021); this shift is also notable, as it is represents a pattern that has likewise been predicted via modelling for Yellowtail Kingfish in Southeastern Australia (Champion et al., 2018). The distinctiveness of AKW otoliths implies partial demographic separation within the NHR, whereas the relative homogeneity among CEW, CHA, and SOU indicates that fish in southern regions likely represent recent or ongoing expansion. The difficulty of correctly classifying individuals from these regions supports the interpretation that southern occurrences are not likely to be long-established stocks.

However, otolith shape may be further strengthened when combined with additional markers to more confidently identify expansion-associated individuals. Integrating contour-based morphology with complementary data would provide a more comprehensive framework. Integrating otolith shape with complementary markers such as stable isotopes or genomic data will aid definitively to achieve the resolution required for fisheries management. Multi-marker approaches have already proven powerful elsewhere: combining shape with stable isotopes has revealed stock boundaries in *Coryphaenoides rupestris* (Longmore et al., 2010) and *Spondyliosoma cantharus* (Neves et al., 2019), while combination with genomic analyses has resolved fine-scale differentiation in high-dispersal marine fish (Pita et al., 2016; Randon et al., 2020). Applying such integrative analyses to Yellowtail Kingfish will be essential for quantifying the degree and persistence of the SRE, clarifying the demographic role of expansion-associated individuals, and understanding their contribution to long-term persistence under climate change.

4.2 Implications for management of Yellowtail Kingfish

From a management perspective, the implications of these findings are important. If SRE fish remain demographically linked to the NHR, treating them as independent units risks underestimating stock size and sustainability. Conversely, the emergence of stable morphological divergence in SRE stocks would signal the formation of new stock components, requiring a revision of management boundaries. Future monitoring of otolith morphology, in combination with genomic and isotopic markers, will be essential to track whether the current southward expansion stabilises into permanent, demographically independent stocks. In summary, this study highlights a two-part structure: a northern component with detectable morphological distinctiveness, the 'NHR', and a morphologically homogeneous expansion front, the 'SRE'. These findings demonstrate the utility of otolith shape to identify "expander" individuals, even in pelagic fishes. This is significant given range expansions are an increasing phenomenon among marine taxa (Pinsky

et al., 2020; Dahms & Killen, 2023), and otolith shape analyses are relatively easy, inexpensive, and non-destructive to monitoring collections.

4.3 Heterogeneity within the Bay of Plenty (BPLE) Group

Multivariate dispersion within the BPLE sampling group was significantly higher than in AKW or CEW, violating the assumption of homogeneity required for PERMANOVA. While this statistical violation complicates inference, especially within the context of the range expansion discussed here, the elevated within-group variation may reflect real biological heterogeneity. The BPLE has previously been described as a transition zone for Kingfish populations; significant meristic variation (e.g. fin ray counts) between eastern and western populations have been reported, and parasite-based markers suggest a potential stock boundary in this region (Smith et al., 2004; McKenzie, 2014). Such findings align with our results and raise the possibility that BPLE may include a mixture of individuals from distinct ecological contexts, warranting further research.

5 Acknowledgments

Te Herenga Waka – Victoria University of Wellington provided financial support for this project. We thank Fisheries New Zealand, Ministry for Primary Industries, New Zealand Government, for granting access to the otoliths and associated metadata. We also acknowledge the team at Earth Sciences New Zealand – Wellington (formerly NIWA), particularly Caoimhghin Ó Maolagáin, for support throughout this work, including providing access to materials and equipment.

6 Author contributions

Carla H. Finn: Formal analysis (lead), investigation (lead), methodology (lead), writing – original draft (lead), writing – review and editing (lead), data curation (lead), visualisation (lead), conceptualisation (equal)
Tom Barnes: supervision (equal), Resources (lead), data curation (supporting), conceptualisation (equal), investigation (supporting)
Maren Wellenreuther: writing - review and editing (supporting), supervision (supporting).
David Chagné: writing - review and editing (supporting), supervision (supporting)
Peter Ritchie: writing - review and editing (supporting), conceptualisation (support), supervision (equal).

References

Anderson, M. J., & Willis, T. J. (2003). Canonical analysis of principal coordinates: A useful method of constrained ordination for ecology. *Ecology*, *84*(2). doi: 10.1890/0012-9658(2003)084[0511:CAOPCA]2.0.CO;2

Aneesh Kumar, K. V., Nikki, R., Oxona, K., Hashim, M., & Sudhakar, M. (2017). Relationships between fish and otolith size of nine deep-sea fishes from the Andaman and Nicobar waters, North Indian Ocean. *Journal of Applied Ichthyology*, *33*(6). doi: 10.1111/jai.13467

Arbizu, P. M. (2020). *pairwiseAdonis: Pairwise multilevel comparison using adonis.*

Berg, F., Almeland, O. W., Skadal, J., Slotte, A., Andersson, L., & Folkvord, A. (2018). Genetic factors have a major effect on growth, number of vertebrae and otolith shape in Atlantic herring (Clupea harengus). *PLoS ONE*, *13*(1). doi: 10.1371/journal.pone.0190995

Cadrin, S. X., Kerr, L. A., & Mariani, S. (2013). Stock Identification Methods: An Overview. In *Stock identification methods: Applications in fishery science: Second edition.* doi: 10.1016/B978-0-12-397003-9.00001-1

Carvalho, G. R., & Hauser, L. (1994). *Molecular genetics and the stock concept in fisheries* (Vol. 4) (No. 3). doi: 10.1007/BF00042908

Champion, C., Brodie, S., & Coleman, M. A. (2021). Climate-Driven Range Shifts Are Rapid Yet Variable Among Recreationally Important Coastal-Pelagic Fishes. *Frontiers in Marine Science*, *8*. doi: 10.3389/fmars.2021.622299

Champion, C., Hobday, A. J., Tracey, S. R., & Pecl, G. T. (2018). Rapid shifts in distribution and high-latitude persistence of oceanographic habitat revealed using citizen science data from a climate change hotspot. *Global Change Biology*, *24*(11). doi: 10.1111/gcb.14398

Clark, F. J. K., da Silva Lima, C. S., & Pessanha, A. L. M. (2021). Otolith shape analysis of the Brazilian silverside in two northeastern Brazilian estuaries with distinct salinity ranges. *Fisheries Research*, *243*. doi: 10.1016/j.fishres.2021.106094

Crandall, C. A. C., Parkyn, D. C., & Murie, D. J. (2013). *Regional stock structure of greater amberjack in the southeastern United States using otolith shape analysis* (Tech. Rep. No. SEDAR33-DW25). North Charleston, SC: SEDAR.

Cryer, M., Mace, P. M., & Sullivan, K. J. (2016, 4). New Zealand's ecosystem approach to fisheries management. *Fisheries Oceanography*, *25*, 57–70. doi: 10.1111/fog.12088

Dahms, C., & Killen, S. S. (2023). *Temperature change effects on marine fish range shifts: A meta-analysis of ecological and methodological predictors* (Vol. 29) (No. 16). doi: 10.1111/gcb.16770

Das, M. (1994). Age determination and longevity in fishes. *Gerontology*, *40*(2-4). doi: 10.1159/000213580

Fisheries New Zealand. (2020, 5). *Proposal to vary the Total Allowable Catch and Total Allowable Commercial Catch for Kingfish (KIN 3).* https://www.nzsportfishing.co.nz/wp-content/uploads/2020/08/KIN-proposal-FNZ-May20.pdf.

Gauldie, R. W., & Crampton, J. S. (2002). An eco-morphological explanation of individual variability in the shape of the fish otolith: Comparison of the otolith of Hoplostethus atlanticus with other species by depth. *Journal of Fish Biology*, *60*(5). doi: 10.1006/jfbi.2002.1938

Geladakis, G., Kourkouta, C., Somarakis, S., & Koumoundouros, G. (2022). Developmental Temperature Shapes the Otolith Morphology of Metamorphosing and Juvenile Gilthead Seabream (Sparus aurata Linnaeus, 1758). *Fishes*, *7*(2). doi: 10.3390/fishes7020082

Hadley Wickham, Romain François, Lionel Henry, & Kirill Müller. (2020). A grammar of data manipulation [R package dplyr version 1.0.0]. *Media*.

Ihssen, P. E., Booke, H. E., Casselman, J. M., McGlade, J. M., Payne, N. R., & Utter, F. M. (1981). Stock Identification: Materials and Methods. *Canadian Journal of Fisheries and Aquatic Sciences*, *38*(12). doi: 10.1139/f81-230

Kassambara, A. (2021). *Pipe-friendly framework for basic statistical tests [R Package 'rstatix' version 0.7. 0].*

Kemp, F. (2003). Modern Applied Statistics with S,. *Journal of the Royal Statistical Society: Series D (The Statistician)*, *52*(4). doi: 10.1046/j.1467-9884.2003.t01-19-00383{_}22.x

Libungan, L. A., Óskarsson, G. J., Slotte, A., Jacobsen, J. A., & Pálsson, S. (2015). Otolith shape: A population marker for Atlantic herring Clupea harengus. *Journal of Fish Biology*, *86*(4). doi: 10.1111/jfb.12647

Libungan, L. A., & Pálsson, S. (2015). ShapeR: An R package to study otolith shape variation among fish populations. *PLoS ONE*, *10*(3). doi: 10.1371/journal.pone.0121102

Lleonart, J., Salat, J., & Torres, G. J. (2000). Removing allometric effects of body size in morphological analysis. *Journal of Theoretical Biology*, *205*(1). doi: 10.1006/jtbi.2000.2043

Longmore, C., Fogarty, K., Neat, F., Brophy, D., Trueman, C., Milton, A., & Mariani, S. (2010). A comparison of otolith microchemistry and otolith shape analysis for the study of spatial variation in a deep-sea teleost, Coryphaenoides rupestris. *Environmental Biology of Fishes*, *89*(3). doi: 10.1007/s10641-010-9674-1

Mahé, K., Gourtay, C., Defruit, G. B., Chantre, C., de Pontual, H., Amara, R., ... Ernande, B. (2019). Do environmental conditions (temperature and food composition) affect otolith shape during fish early-juvenile phase? An experimental approach applied to European Seabass (Dicentrarchus labrax). *Journal of Experimental Marine Biology and Ecology*, *521*. doi: 10.1016/j.jembe.2019.151239

McKenzie, J. R. (2014). Review of productivity parameters and stock assessment options for kingfish (Seriola lalandi lalandi). *New Zealand Fisheries Assessment Report*.

Mille, T., Mahé, K., Cachera, M., Villanueva, M. C., De Pontual, H., & Ernande, B. (2016). Diet is correlated with otolith shape in marine fish. *Marine Ecology Progress Series*, *555*. doi: 10.3354/meps11784

Ministry for Primary Industries. (2019). New Zealand Government Aquaculture Strategy. *Aquaculture Strategy*.

MPI. (2002). *Kingfish QMAs, Geospatial Management, Ministry for Primary Industries.* Retrieved from `https://data-mpi.opendata.arcgis.com/datasets/MPI::kingfish-qmas-1/about`

Nazir, A., & Khan, M. A. (2021). Using otoliths for fish stock discrimination: Status and challenges. *Acta Ichthyologica et Piscatoria*, *51*(2). doi: 10.3897/aiep.51.64166

Ndjamba, T. S. I., Araya, M., & Oliva, M. E. (2022). Otolith Weight as an Estimator of the Age of Seriola lalandi Valenciennes, 1833 (Carangidae), in the Southeastern Pacific. *Animals*, *12*(13). doi: 10.3390/ani12131640

Neves, A., Vieira, A. R., Sequeira, V., Paiva, R. B., Janeiro, A. I., Gaspar, L. M., & Gordo, L. S. (2019). Otolith shape and isotopic ratio analyses as a tool to study Spondyliosoma cantharus population structure. *Marine Environmental Research*, *143*. doi: 10.1016/j.marenvres.2018.11.012

Oksanen, J., Blanchet, F. G., Kindt, R., Legendre, P., Minchin, P. R., O'Hara, R. B., ... Wagner, H. (2016). vegan: Community Ecology R Package, version 2.6-4. *vegan: Community Ecology Package. R package version 2.4-1. https://CRAN.R-project.org/package=vegan*, *8*(December).

Park, J. M., Kang, M. G., Kim, J. H., Jawad, L. A., & Majeed, S. (2023). Otolith morphology as a tool for stock discrimination of three rockfish species in the East Sea of Korea. *Frontiers in Marine Science*, *10*. doi: 10.3389/fmars.2023.1301178

Pinsky, M. L., Selden, R. L., & Kitchel, Z. J. (2020). *Climate-Driven Shifts in Marine Species Ranges: Scaling from Organisms to Communities* (Vol. 12). doi: 10.1146/annurev-marine-010419-010916

Pita, A., Casey, J., Hawkins, S. J., Villarreal, M. R., Gutiérrez, M. J., Cabral, H., ... Presa, P. (2016). *Conceptual and practical advances in fish stock delineation* (Vol. 173). doi: 10.1016/j.fishres.2015.10.029

Poloczanska, E. S., Brown, C. J., Sydeman, W. J., Kiessling, W., Schoeman, D. S., Moore, P. J., ... Richardson, A. J. (2013). Global imprint of climate change on marine life. *Nature Climate Change*, *3*(10). doi: 10.1038/nclimate1958

R Core Team. (2019). *R: A language and environment for statistical computing.*

Randon, M., Le Pape, O., Ernande, B., Mahé, K., Volckaert, F. A., Petit, E. J., ... Réveillac, E. (2020). Complementarity and discriminatory power of genotype and otolith shape in describing the fine-scale population structure of an exploited fish, the common sole of the Eastern English Channel. *PLoS ONE*, *15*(11 November). doi: 10.1371/journal.pone.0241429

Schneider, C. A., Rasband, W. S., & Eliceiri, K. W. (2012). *NIH Image to ImageJ: 25 years of image analysis* (Vol. 9) (No. 7). doi: 10.1038/nmeth.2089

Smith, P. J., Diggles, B., McKenzie, J., Kim, S., Ó˜Maolagáin, C., & Notman, P. (2004). *Kingfish Stock Structure: Final Research Report for Ministry of Fisheries Project KIN2002/01, Objective 1* (Tech. Rep.). Ministry of Fisheries, New Zealand.

Vignon, M., & Morat, F. (2010). Environmental and genetic determinant of otolith shape revealed by a non-indigenous tropical fish. *Marine Ecology Progress Series*, *411*. doi: 10.3354/meps08651

Waples, R. S., & Gaggiotti, O. (2006). *What is a population? An empirical evaluation of some genetic methods for identifying the number of gene pools and their degree of connectivity* (Vol. 15) (No. 6). doi: 10.1111/j.1365-294X.2006.02890.x

Wickham, H. (2011). ggplot2. *Wiley Interdisciplinary Reviews: Computational Statistics*, *3*(2). doi: 10.1002/wics.147

Wickham, H., Vaughan, D., & Girlich, M. (2024). *tidyr: Tidy Messy Data* (Vol. 59) (No. 10).

Appendices

Appendix - Figures

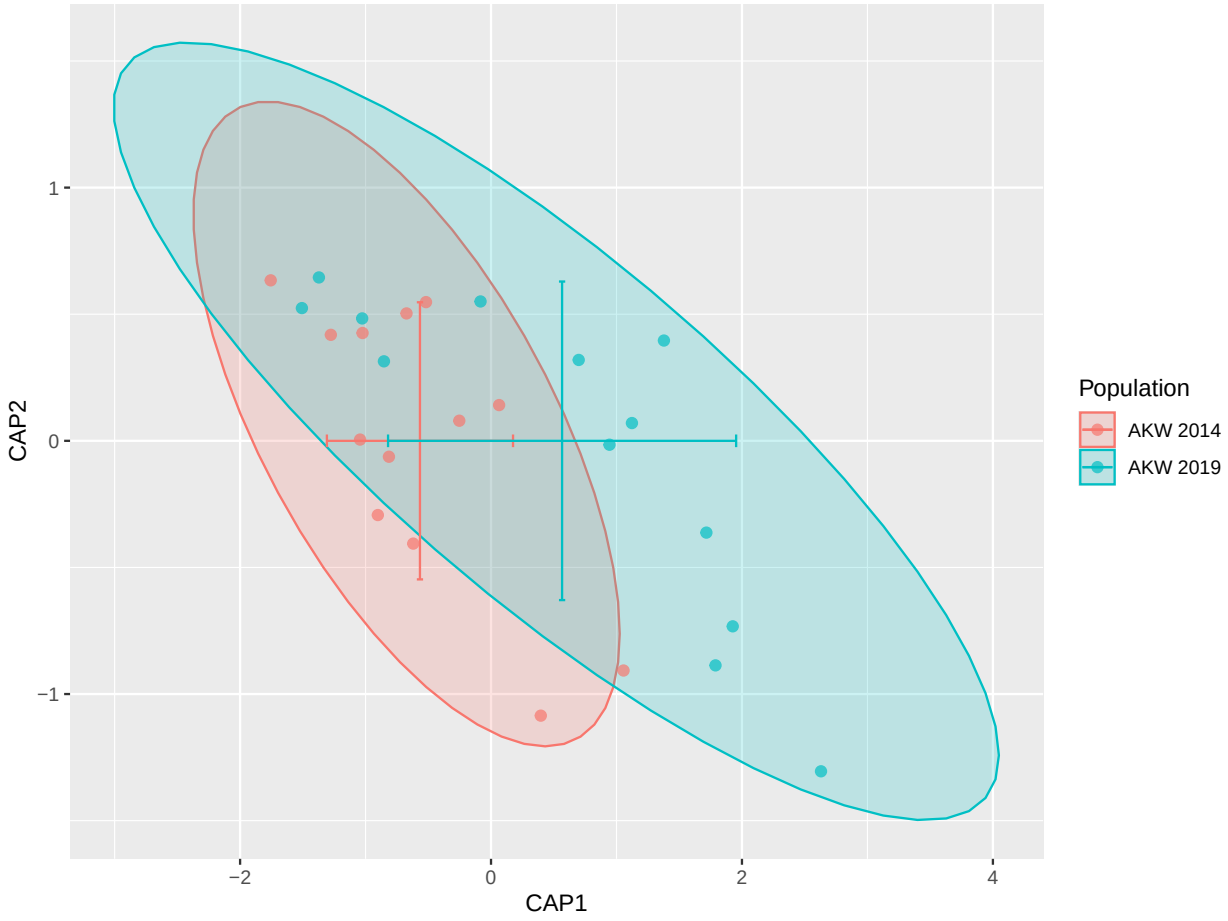

Figure S1: CAP ordination plot of AKW otolith shapes (2014 vs 2019). Ellipses indicate 95% confidence regions based on multivariate normality.

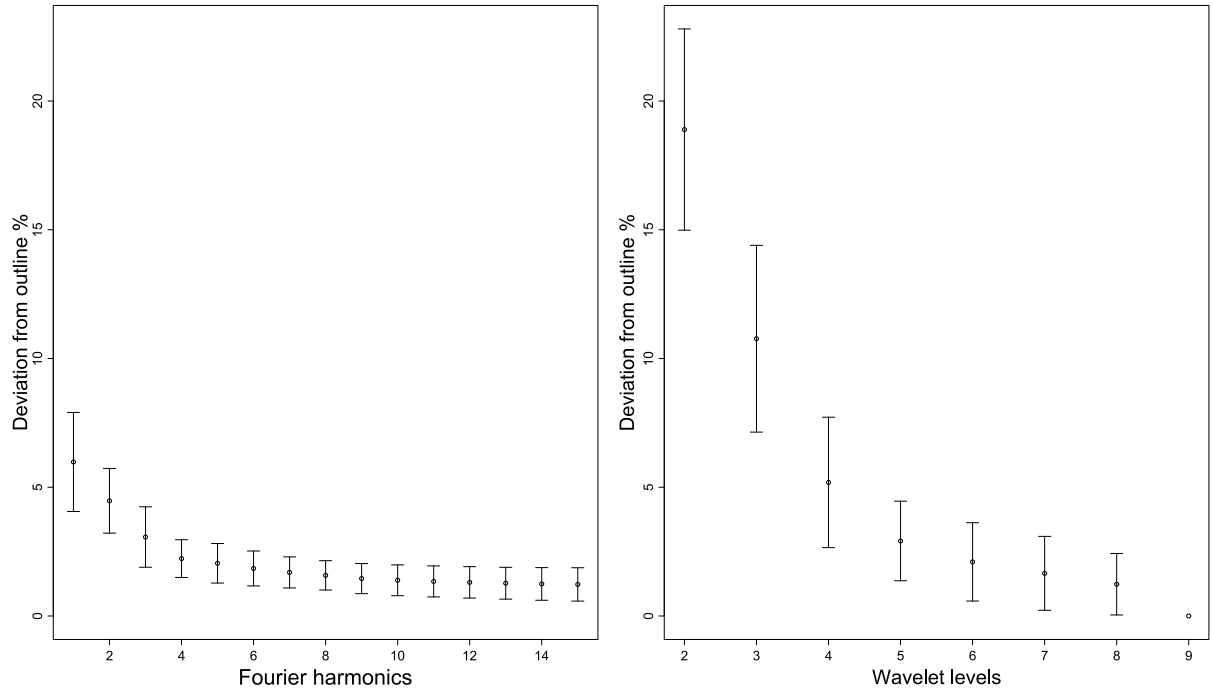

Figure S2: Mean deviation from the original outline (%) as a function of the number of Fourier harmonics (left), and the number of wavelet levels (right), used in shape reconstruction.

Appendix - Tables

Shape index	**Mean left**	**Mean right**	**Shapiro-Wilk p**	**Test type**	**Holm-adjusted p**
Aspect Ratio	2.8418	2.7611	0.6053	Paired t-test	0.1722
Circularity	32.7173	33.1144	0.0188	Wilcoxon signed-rank	0.7904
Ellipticity	0.4774	0.4657	0.8750	Paired t-test	0.1722
Form Factor	0.3890	0.3833	0.0542	Paired t-test	1.0000
Rectangularity	0.5864	0.5853	0.3877	Paired t-test	1.0000
Roundness	0.2644	0.2719	0.3360	Paired t-test	0.3095

Table S1: Comparison of left and right otolith shape indices. Normality assessed using the Shapiro-Wilk test. Holm-adjusted p-values indicate no significant asymmetry.

Shape index	**F-value**	**p-value**	**Holm-adjusted p**
Aspect Ratio	0.066	0.7979	1.0000
Circularity	0.005	0.9425	1.0000
Ellipticity	0.085	0.7711	1.0000
Form Factor	0.000	0.9874	1.0000
Rectangularity	0.073	0.7879	1.0000
Roundness	0.004	0.9481	1.0000

Table S2: ANCOVA interaction effects of side and fish length on otolith shape indices. Holm-adjusted p-values indicate no significant interaction.

Group comparison	**Diff**	**Holm-adjusted p**	**Significant**
BPLE-AKW	0.572	0.00062	*
CEW-AKW	0.107	0.96167	
CHA-AKW	0.220	0.42287	
SOU-AKW	0.395	0.12787	
CEW-BPLE	-0.465	0.03777	*
CHA-BPLE	-0.352	0.06461	
SOU-BPLE	-0.177	0.83273	
CHA-CEW	0.113	0.94627	
SOU-CEW	0.288	0.53218	
SOU-CHA	0.175	0.81155	

Table S3: Pairwise Tukey's HSD comparisons of multivariate dispersion (distance to group centroid). Values show difference in dispersion (Diff) and Holm-adjusted p-values. Significant values indicate heterogeneity in within-group variance.